Passive cooling performance of a test room equipped with normal and new designed Trombe walls: A numerical approach

Mehran Rabani[a, *]

m.rabani@ardakan.ac.ir

Vali Kalantar[b]

vkalantar@yazd.ac.ir

Mehrdad Rabani[c, d]

mehrab@oslomet.no, mehrdadr@stud.ntnu.no

[a]Department of Mechanical Engineering, Faculty of Engineering, Ardakan University, P.O. Box 184, Ardakan, Iran

[b]Department of Mechanical Engineering, Yazd University, Yazd, Iran

[c]Department of Civil Engineering and Energy Technology, OsloMet – Oslo Metropolitan University, Norway

[d]Department of Energy and Process Engineering, Norwegian University of Science and Technology, Norway

*Corresponding author.

Abstract

This paper is dedicated to numerically appraise the passive cooling performance of the new designed and normal Trombe walls combined with solar chimney and water spraying system (WSS) in a test room under Yazd (Iran) desert climate. The new designed Trombe wall expands the indoor space and decreases the implementation cost of the Trombe wall. Furthermore, it can receive the solar intensity from three directions while the normal Trombe wall can only receive it from one direction. The numerical simulation of the new designed Trombe wall was validated by the previous experimental study. The present numerical results indicate that in the morning the average room temperature in the new designed Trombe wall is lower than the normal type since the new designed Trombe wall generates higher natural air ventilation compared with the normal type. But, in the late hour of the day due to the more expansive area of normal Trombe wall and its higher capability to store the solar thermal energy, the average room temperature decreases to a greater extent in the normal type. Moreover, the cooling efficiency analysis demonstrates that the daily average cooling efficiency of the new designed Trombe wall surpasses the normal type by around 8.63%.

Keywords: New designed Trombe wall; Solar intensity; Water spraying system; Cooling efficiency; Passive cooling

Nomenclature

C_{pf}

specific heat of airflow at constant pressure (J/kg.K)

D_{H_2o}

diffusion coefficient of water vapor into air (m^2/s)

E

energy term (J)

g

acceleration gravity (m/s^2)

h_a

convective heat transfer coefficient of ambient (W/m^2.K)

K

thermal conductivity (W/m.K)

m

mass of concrete (kg)

$\dot{m}$

mass flow rate (kg/s)

P

static pressure (Pa)

Q_0

heat transferred to the air flow in the channel (W)

Q_r

solar intensity received by absorber (W)

Q_{tot}

total heat (W)

S_{ct}

turbulent Schmidt number

S_{H_2o}

water vapor added to or removed from the air (kg/s.m^2)

T

temperature (K)

T_0

operating temperature (K)

t

time (s)

u_i, u_j

direction velocity (m/s)

V_a

outdoor velocity (m/s)

x_i, x_j

cartesian directions

Y_{H_2o}

mass fraction of species

Greek symbols

γ

mean temperature approximation coefficient

ρ

air density (kg/m^3)

ρ_c

concrete density (kg/m^3)

ρ_0

density of the flow (kg/m^3)

β

thermal expansion coefficient

η

cooling efficiency

μ

dynamic viscosity (Pa.s)

μ_t

turbulent dynamic viscosity (Pa.s)

Introduction

Saving energy and sustainable development are two key factors in building constructions. Approximately 30% of the total world energy is consumed for heating and cooling of buildings [1]. Natural ventilation and renewable energy applications are widely used to improve the indoor air environment and reduce the energy consumption of air conditioning systems.

Passive systems are widely employed in the arid cities such as Yazd (Iran) (Fig. 1) in order to optimize the energy and reduce the costly mechanical systems in residential areas. One of the passive systems is Trombe wall that mostly implemented for heating applications.

Fig. 1 Natural cooling using double wind tower and cistern in a traditional building in Yazd (Iran).

Due to the fact that the Trombe wall system was originally conceived for cold climates, there is a large body of research studying its winter performance. These researches commonly dealt with the performance of Trombe walls with 20 cm thickness of concrete wall [2–4], the effect of different parameters such as different Trombe wall materials [5,6], various dimensions of channel and vents of the Trombe wall [7,8], and different width of the Trombe wall [9,10] on the stored energy, average room temperature, and comfortable conditions. In spite of its widespread winter application, making use of this system in summer can lead to an undesired energy transfer and overheating phenomena especially in the well insulated buildings [11]. Only few studies have focused on summer performance [12]. Practically, adopting a hybrid passive system such as integration of Trombe wall system with solar chimney can reasonably justify the use of Trombe wall for summer applications.

The solar chimney is an effective method to enhance the space natural ventilation. In most tropical countries, where it is almost very difficult to implement an air conditioner, people rely on natural ventilation, instead, to achieve comfort through opening windows [13].

Different studies investigated the solar chimney features such as the effect of chimney dimensions on its performance [14–17].

A very effective method in defining the performance of such passive solar systems is analytical approach. In this regard, many authors analytically studied the performance of solar chimneys [18,19]. Zamora and Kaiser also analytically examined the optimal ratio (ratio of width to length of channel) of solar chimney [20]. The optimal ratio accounts for maximum average Nusselt number on the walls and mass flow rate inside the channel. Their results revealed that the increase of Rayleigh number decreases the optimal ratio in laminar flows with isothermal boundary condition.

Sometimes solar chimney is unable to properly provide comfortable condition inside the buildings. Thus, its integration with other devices such as water spraying system (WSS) can improve its performance. Employing natural or passive cooling system can be an alternative way to maintain a cool house or reduce air-conditioning load [21].

Solar cooling can be implemented through different ways. A simple and practical way is adopting appropriate insulation materials to building envelope which can establish a desirable condition inside the room [22]. In another way, the water spraying system (WSS) can be integrated with natural air ventilation devices inside the buildings to benefit from passive cooling [23–26].

In the present study, the main intention is to numerically compare the cooling performance of the new designed Trombe wall with that of normal type in order to reduce the implementation and construction costs of normal type and improve the Trombe wall performance simultaneously. It is worth mentioning that the heating performance of the new designed Trombe wall system in winter and its cooling performance in summer, using its combination with solar chimney and WSS, were experimentally studied in our previous studies [27].

Modeled case

Geometry specification

The new designed Trombe wall model (all system dimensions shown in Table 1) was considered based on its empirical one [27], which is shown in Fig. 2. In addition, all optimum dimensions of the Trombe wall system were selected based on the previous works in order to provide the best cooling performance and natural convection in the room

Table 1 Optimum dimensions of the Trombe wall system.

Optimum dimensions	Relevant references

Concrete Trombe wall thickness (new and normal type): 20 cm	[2,27–30]
New designed Trombe wall width: 1 m	[10,27]
Normal Trombe wall width: 2 m	[2,6,11,27–30]
Channel width (new and normal type): 30 cm	[4,7,9,12,27,28]
Upper and lower vent dimensions of Trombe wall (new and normal type): 30 × 50 cm²	[4,7,9,12,27,28]
Inlet and outlet dimensions of solar chimney (new type): 30 × 50 cm²	[14–19,27]
Inlet and outlet dimensions of solar chimney (normal type): 30 × 100 cm²	[14–19,27]
Height of solar chimney (new and normal type): 1 m	[14–19,27]
Dimensions of incoming fresh air ports to the room: 30 × 50 cm²	[27]

(a)
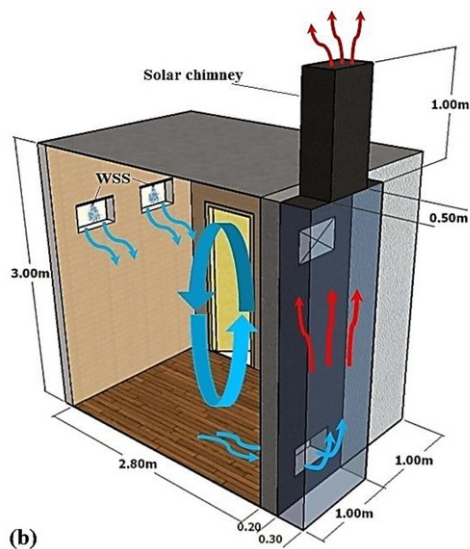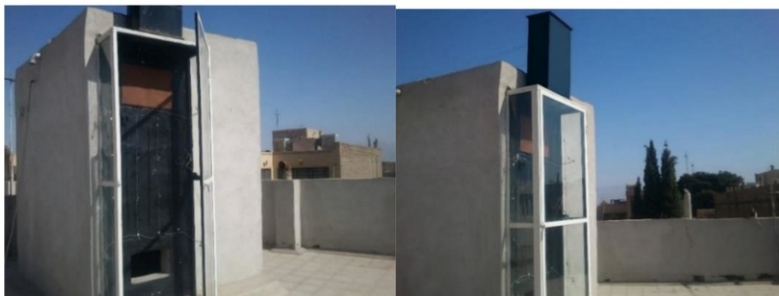
(b)

Fig. 2 (a) Empirical model of test room and the Trombe wall with the new design [27] (b) Schematic of airflow circulation during the cooling performance of the system.

The normal Trombe walls can only receive the solar intensity from one direction (South direction) (Fig. 3a), but in the new designed Trombe wall the side walls of the channel are replaced with the glass. Consequently, the

absorber can receive the solar intensity from three directions (East, West and South directions) (Fig. 3b). Furthermore, with regard to the study of Jaber and Ajib [10], the optimal area ratio of the new designed Trombe wall is considered to be 50% (Fig. 3b) whereas the normal type occupies the whole South wall area (area ratio is 100%) (Fig. 3a).
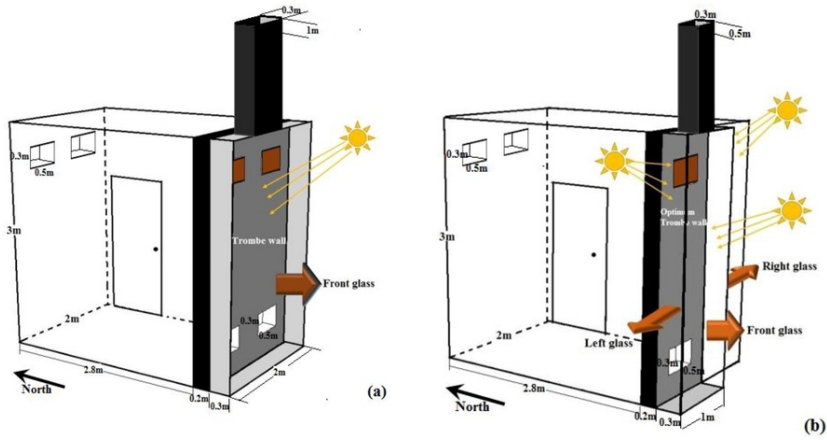

Fig. 3 Schematic of (a) normal Trombe wall and (b) new designed Trombe wall.

The dimensions of the test room in both new designed and normal Trombe walls were considered to be $3\,\text{m} \times 2\,\text{m} \times 3\,\text{m}$ and the dimensions of other parts of the Trombe wall were selected according to the best thermal performance of the system (Table 1). Furthermore, two incoming fresh airports were applied symmetrically on the back wall of the room (North side). The distance between the ports and the ceiling is 40 cm, and the distance between the ports is 35 cm. In order to achieve the optimal cooling performance, it is necessary to completely isolate the room with appropriate materials. The basic properties of the materials to reach this efficiency have been provided in Table 2 (Fig. 4).

Table 2 Material properties.

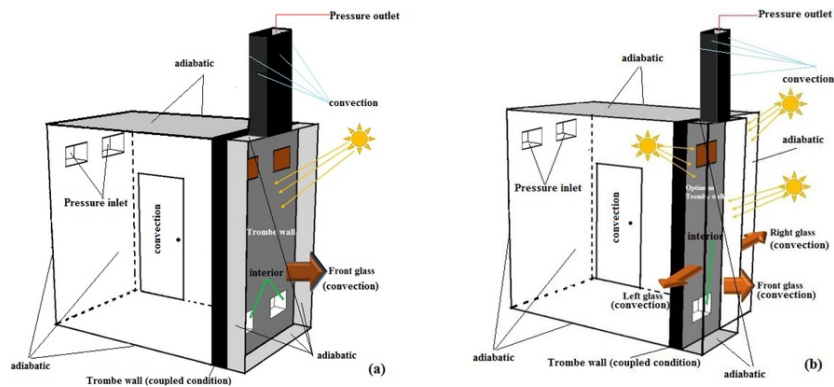| Material	Density (kg/m³)	Specific heat (J/kg.K)	Thermal conductivity (W/m.K)	Emissivity Coefficients
Concrete	2100	840	1.5	0.92
Glass	2500	750	1.4	0.95
Wood	700	2310	0.173	0.88
Stainless steel	8000	500	15	0.8

Fig. 4 Boundary contions of (a) normal Trombe wall and (b) new designed Trombe wall.

Boundary conditions

The boundary conditions for numerical simulations were applied based on the empirical study. The insulated boundary condition was adopted for all walls including the side walls, the ceiling and the floor of the test room, back of the Trombe wall and the floor of the channel in both types of Trombe wall and the side walls of the channel in the normal Trombe wall. The Trombe wall was made of concrete and the coupled thermal condition was considered as its absorber boundary condition. The solar chimney was made of stainless steel. For the solar chimney walls and the glassy parts of the channel in both types of Trombe wall, the convection boundary condition was selected. The same boundary condition was also employed for the wooden room door (Fig. 4). The convection boundary condition was characterized by the outdoor condition, which has been considered based on the experimental data [27] in one day in Yazd (30 June 2015) as shown in Fig. 5. The ambient air temperature has been input to the software by UDF. The convection heat transfer coefficient was calculated based on the Eq. (1) [13,18,19,21].

$$h_a = 2.8 + 3V_a \qquad (1)$$

where V_a is the average air velocity, which was chosen based on the climatic data on the 30 June. The average amount of outdoor convection heat transfer coefficient was obtained by around 11.2 W/m^2 K.
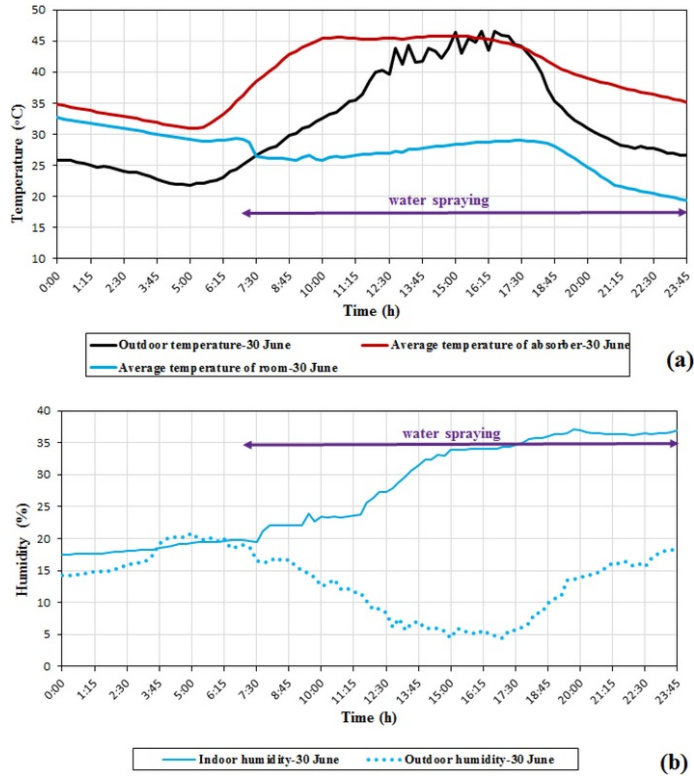

Fig. 5 Variation of (a) temperature (b) relative humidity in different parts with WSS for 30 June 2015 [27].

The solar radiation on the absorber was modeled by the solar ray tracing. The solar load model's ray tracing algorithm can be used to predict the direct illumination energy source that results from incident solar radiation. In addition, based on the measurements have been made using the solar power meter (TES-1333R) in the experimental work, the absorptivity coefficient was considered to be 0.95 [27].

The humid condition used in the present study was modeled based on the water spraying model already implemented in ANSYS-FLUENT software. The details of the parameters required for the simulation of the water spraying system were as follows (Table 3):

   (1) The "Species Transport Model" was selected.

Define > Models > Species > Transport & Reaction > Species Transport

(2) Based on the number of inlet ports, the number of injections were selected

Define > Injections > Create Injections > Set Injection properties

Furthermore, regarding the problem conditions, the parameters in the "Point Properties" section including diameter, temperature, velocity magnitude, and total flow rate were determined.

The water spraying system parameters were selected with regard to the experimental conditions [27]. According to the Adaptive Comfort Standard (ACS) evaluation as well as the optimum water mass flow rate and water droplet diameter in the experimental work, the mass flow of 10 l/h and the water droplet diameter of 30 μm were chosen. The water temperature in WSS was considered to be 20 °C.

Governing equations

The flow in the Trombe wall system is governed by the unsteady state and turbulence form (k- ε turbulence model) of the fluid flow conservation equations that include averaged Navier-Stokes equations in conjunction with the total energy equation. Since the velocities in the natural convection are low, the viscous stress term in the energy equation has been ignored, and the flow is considered to be incompressible. The buoyancy force is modeled by Boussinesq approximation. The governing equations can be written in their compact Cartesian form as follows:

- Continuity equation

The continuity equation governing the flow, take the form:

$$\frac{\partial \rho}{\partial t} + \frac{\partial (\rho u_i)}{\partial x_i} = 0 \tag{2}$$

- Momentum equation

The Reynolds-averaged Navier-Stokes equations governing the flow, take the form:

$$\frac{\partial}{\partial t}(\rho u_i) + \frac{\partial}{\partial x_j}(\rho u_i u_j) = -\frac{\partial P}{\partial x_i} + \frac{\partial}{\partial x_j}\left[\mu\left(\frac{\partial u_i}{\partial x_j} + \frac{\partial u_j}{\partial x_i} - \frac{2}{3}\delta_{ij}\frac{\partial u_l}{\partial x_l}\right)\right] + \rho g_i + \frac{\partial}{\partial x_j}\left(-\overline{\rho u_i' u_j'}\right) - \overline{\rho u_i' u_j'} = \mu_t\left(\frac{\partial u_i}{\partial x_j} + \frac{\partial u_j}{\partial x_i}\right) - \frac{2}{3}\left(\rho k + \mu_t\frac{\partial u_k}{\partial x_k}\right)\delta_{ij} \tag{3}$$

Since the flow is buoyancy-driven the term ρg_i in Eq. (3) is carried out by the Boussinesq's model for the vertical direction as follows:

$$(\rho - \rho_0)\,\text{g} \cong -\rho_0 \beta\,(\text{T} - \text{T}_0)\,\text{g} \tag{4}$$

- Energy equation

For the temperature distribution calculations, the energy equation can be written as [24]:

$$\frac{\partial(\rho E)}{\partial t} + \frac{\partial}{\partial x_i}\left[u_i\left(\rho E + P\right)\right] = \frac{\partial}{\partial x_j}\left[k_{eff}\frac{\partial T}{\partial x_j} + u_i(\tau_{ij})_{eff}\right]$$
$$k_{eff} = K + \frac{C_P \mu_t}{\text{Pr}_t},\ \ (\tau_{ij})_{eff} = \mu_{eff}\left(\frac{\partial u_i}{\partial x_j} + \frac{\partial u_j}{\partial x_i}\right) - \frac{2}{3}\left(\mu_{eff}\frac{\partial u_k}{\partial x_k}\right)\delta_{ij} \tag{5}$$

- Species Transport Equation

The species transport equation of water vapor into air is written in the form [24]:

$$\frac{\partial}{\partial t}\left(\rho Y_{H_2O}\right) + \frac{\partial}{\partial x_j}\left(\rho Y_{H_2O}\,u_i\right) = \frac{\partial}{\partial x_j}\left[\left(\rho D_{H_2O} + \frac{\mu_t}{sc_t}\right)\frac{\partial Y_{H_2O}}{\partial x_j}\right] + S_{H_2O} \tag{6}$$

where S_{H_2o} is the water vapor added to or removed from the air due to evaporation or condensation. The constant D_{H_2o} is the diffusion coefficient of water vapor into air, which is equal to 2.88×10^5; Sc_t is the turbulent

Schmidt number, which is equal to 0.7 and Y_{H_2o} is the mass fraction of water vapor.

In the current study, the governing equations were discretized using the finite volume method. A commercial CFD code (ANSYS–FLUENT 15.0) was employed in this numerical investigation. The whole discretization method was based on high accuracy models for this solution. The solver type was pressure-based because of natural convection. In solution method, the flow was considered to be incompressible and PISO algorithm with skewness correction of 1 and neighbor correction of 4 was adopted for pressure and velocity coupling. In addition, in the spatial discretization, the pressure was discretized with PRESTO model and momentum, turbulent kinetic energy, turbulent dissipation rate and energy were discretized with second order upwind model. The transient formulation was discretized based on second order implicit model.

The convergence absolute criteria for continuity, x-velocity, y-velocity and z-velocity is 10^{-4}, for energy is 10^{-7}, and for k and ε is 10^{-4}.

Result and discussion

The results have been presented in different parts of the room for different parameters. The first part of the results includes the validation of numerical results by the experimental data [27]. The second part describes the temperature variation in different parts and the third part illustrates the indoor relative humidity variation. The fourth part investigates the velocity variation in the vents and the channel and the next part analyzes the stored energy within the Trombe wall. The final part of the results compares the cooling efficiency of the normal and the new designed Trombe wall.

Grid sensitivity and validation

A non–uniform hexahedral mesh has been considered for numerical simulations (Fig. 6). Four different grids with 1.7×10^6, 2.1×10^6, 2.5×10^6, and 3×10^6 cells were selected for the Trombe wall with the new channel design and five various grids with 2×10^6, 2.5×10^6, 3×10^6, 3.3×10^6, and 3.5×10^6 cells were applied for the normal Trombe wall (Fig. 7). The variation of average absorber temperature and average room temperature was evaluated for different grid numbers. The maximum discrepancy of room and absorber temperatures for the grids of 2.5×10^6 and 3×10^6 for the Trombe wall with the new channel design and the grids of 3.3×10^6 and 3.5×10^6 for the normal Trombe wall was lower than 1% (Fig. 7). Therefore the grids of 2.5×10^6 and 3.3×10^6 were employed for the new designed and normal Trombe walls, respectively.
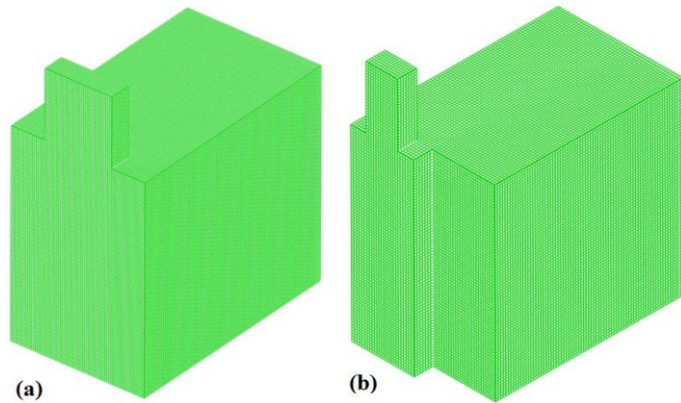

Fig. 6 Computational domain Grid generation for (a) normal and (b) new designed Trombe walls.
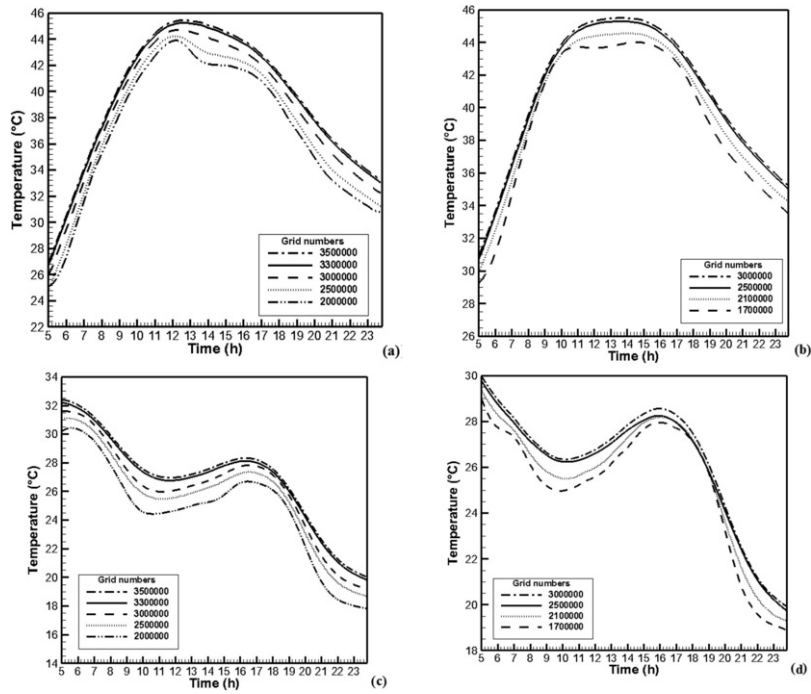
Fig. 7 Absorber temperature variation for different grid numbers for (a) normal Trombe wall and (b) new designed Trombe wall and Test room temperature variation for different grid numbers for (c) normal Trombe wall and (d) new designed Trombe wall.

The results have been analyzed for the day of 30 June 2015. Firstly, the results of numerical simulation of the new designed Trombe wall for the absorber and room temperatures as well as the air velocity inside the channel have been compared and validated by the experimental data [27]. Comparison of results demonstrates the close variation trend between the experimental data and numerical results (Fig. 8).
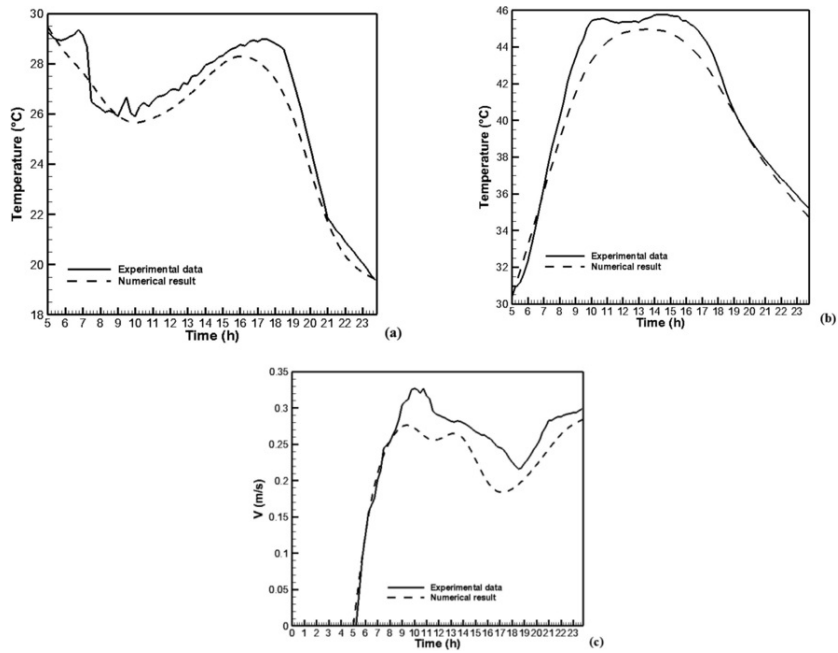
Fig. 8 Comparison of numerical and experimental results [27] for the variation of (a) test room temperature and (b) absorber temperature and (c) air velocity passing through the channel for the new designed Trombe wall.

Afterwards, the variation of temperature, relative humidity and air velocity in different sections of the system and the thermal energy stored within the Trombe wall have been studied. Based on the sensor positions (Fig. 9) in the experimental study [27], several points and sections have been considered inside the room for numerical simulation, which were shown in the Fig. 10.
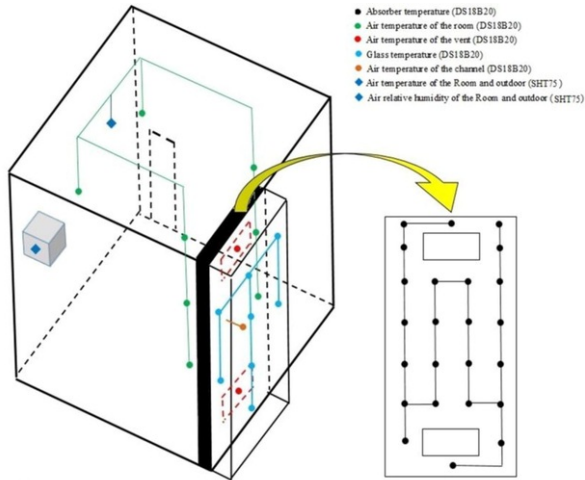

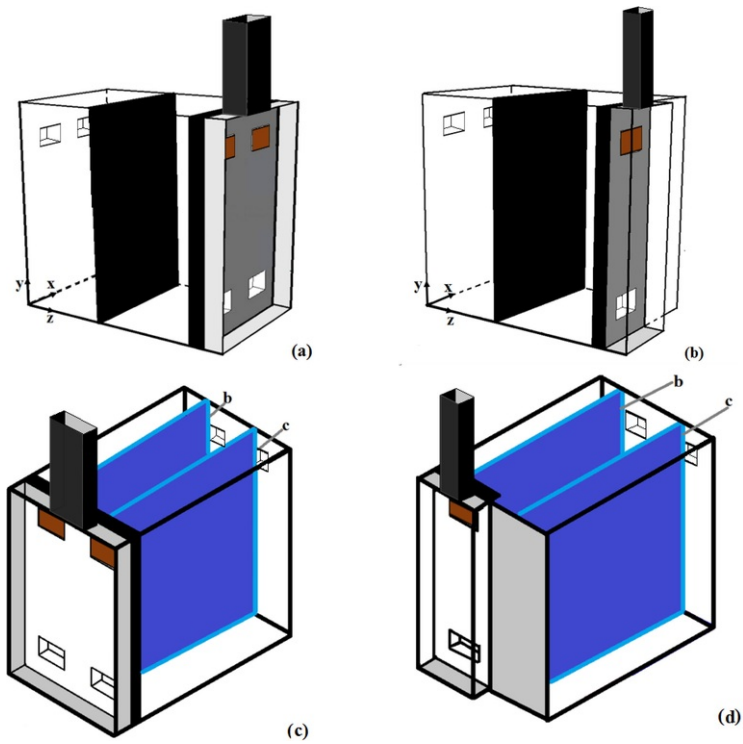**Fig. 9** Sensor positions in the different parts of the system in experimental study [27].

Fig. 10 Cross section a in the middle of the room (z = 1.5 m) for (a) normal and (b) new designed Trombe walls and Cross sections b (x = 0.5 m) and c (x = 1.5 m) inside the room for (c) normal and (d) new designed Trombe walls.

Temperature variation

Fig. 11a indicates the absorber temperature variation. In the morning (5–8), the absorber temperature in the new designed Trombe wall is higher than that in the normal type since the new channel design (replacing wall with glass) enables the absorber to receive solar intensity from the right side of the channel. Same incident happens in the afternoon (17–24) because the absorber of new designed Trombe wall receives the solar intensity from the left side of the channel. In the midday, due to more expansive absorber area, the normal type receives higher solar intensity than the new designed Trombe wall resulting in higher absorber temperature in the normal type absorber. Overall, the average absorber temperature in the new designed Trombe wall is higher than that in the normal type.
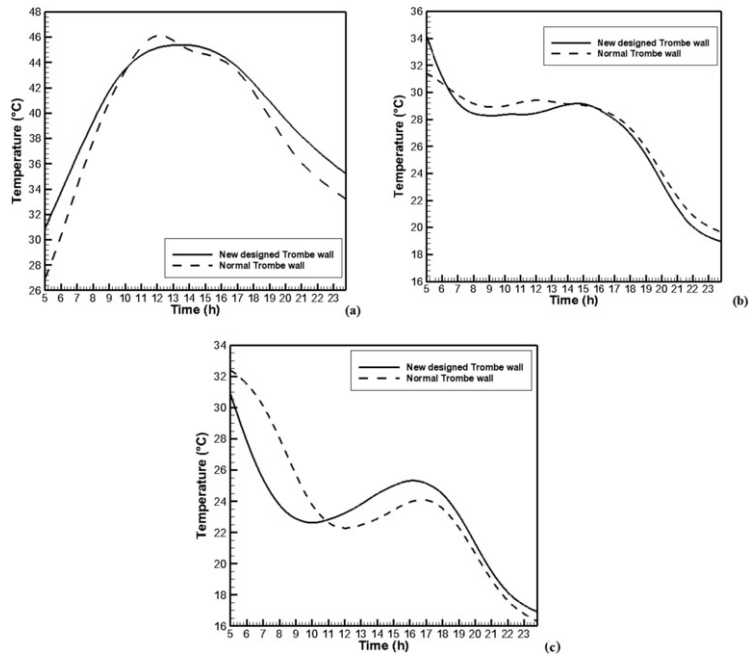
Fig. 11 Average temperature variation of (a) absorber (b) channel and (c) the Trombe wall vent for two Trombe wall types.

Fig. 11b and 11c demonstrate the average temperature variation in the channel and the lower vent of the Trombe wall, respectively. The trend of temperature variation in these parts is almost the same due to the natural convection inside the channel and passing of airflow through the vent. The performance analysis of new designed and normal Trombe walls reveals that the temperature variation of the Trombe wall vent and the channel directly is related to the solar intensity received by the absorber and its increase/decrease leads to increase/decrease of temperature in these parts. Employing WSS in the incoming fresh air ports decreases the temperature inside the test room which in turn decreases the temperature of the Trombe wall vent and the channel.

Comparison of two system types indicates that the channel temperature is nearly the same for two types. But, the normal Trombe wall vent temperature is higher than that of the new designed type in 7–14o'clock due to the higher vent air velocity of the new designed type (Fig. 15), resulting in more air ventilation and temperature decrease in the new designed Trombe wall vent (Table 3).

Table 3 Injection properties in the present study.

Injection Type	Surface
Particle Type	Droplet
Material	Water-Liquid
Diameter Distribution	Uniform
Evaporating Species	H_2O

Fig. 12 demonstrates average temperature variation in three sections (Fig. 10) of the test room. In all sections, the average temperature in the new designed Trombe wall is lower than the normal type in 7–14o'clock because the new designed Trombe wall generates more natural air ventilation resulting in the average room temperature to decrease to a higher extent. In the late hour of the day, due to the more expansive area of the normal Trombe wall and its higher capability to store the solar thermal energy and to transfer this energy to the channel, the air velocity, therefore, natural ventilation in the normal Trombe wall is higher than the new designed type which it in turn causes the average room temperature to decrease to a greater extent. Additionally, the average temperature has been shown in three sections of the test room during the day in Table 4. As might be expected, the average room temperature in the new designed Trombe wall is lower than the normal type by around 2 °C.
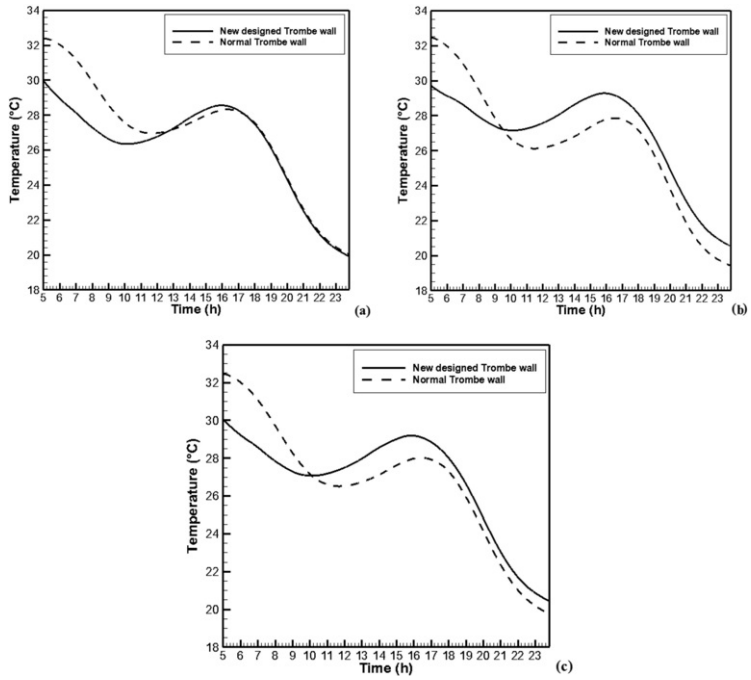
Fig. 12 Average temperature variation of the test room in sections (a) a, (b) b and (c) c for two Trombe wall types.

Table 4 Average temperature in different sections of the test room for two Trombe wall types.

	Type of the Trombe wall	Average room temperature (°C)
Section a	New design	25.1
	Normal	27
Section b	New design	25.8
	Normal	26.4
Section c	New design	25.6
	Normal	26.7

Current indoor conditions were evaluated according to the Adapted Comfort Standard (ACS) specified for thermal comfort in ventilated buildings [31]. Based on the ACS assessment, the thermal comfort conditions for both new designed and normal Trombe walls in the section a have been illustrated in Fig. 13. Both types of the Trombe wall satisfy the indoor thermal comfort. The new designed Trombe wall leads to approximately lower average temperature inside the room.
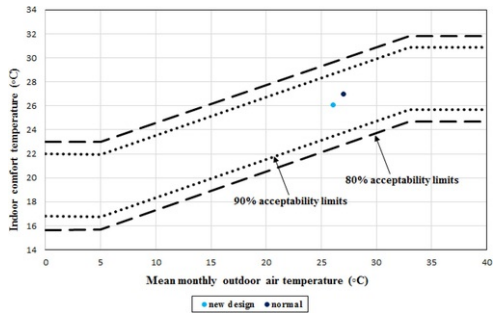
Fig. 13 ACS in section a for two Trombe wall types.

Relative humidity variation

Fig. 14 indicates the relative humidity variation in different room sections. In both types of the Trombe wall, the variation of relative humidity is almost the same. However, the amount of relative humidity in the new designed Trombe wall is slightly greater than the normal type due to the fact the airflow velocity in the new designed Trombe wall is higher than the normal one especially in the morning (Fig. 15). The average relative humidity has been also indicated in the Table 5. In the both types, the amount of relative humidity in the sections b and c is higher than the section a since these sections were located in the vicinity of the WSS situated on the incoming fresh air ports.
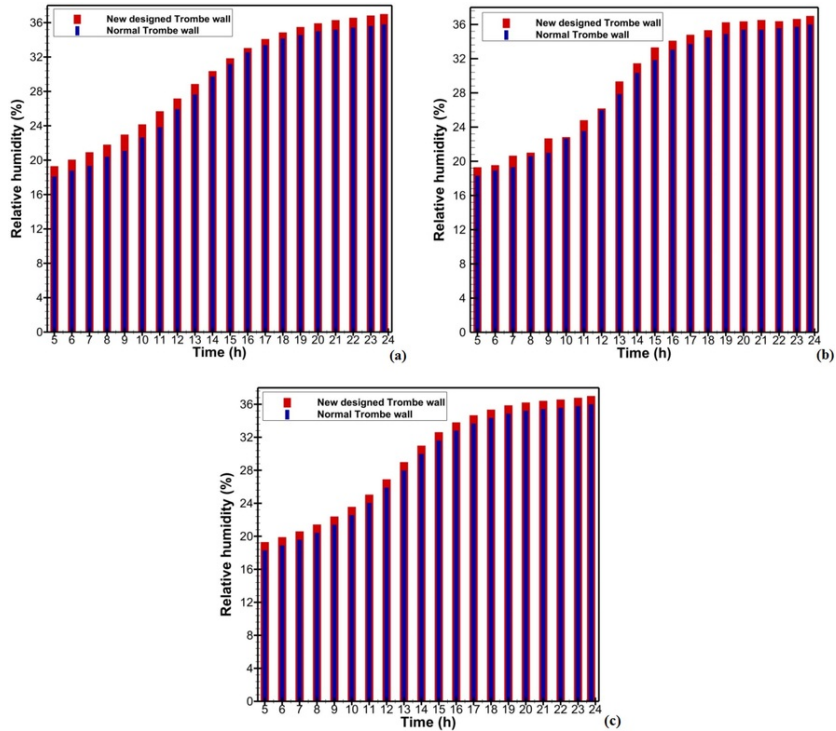

Fig. 14 Average relative humidity variation of the test room in sections (a) a, (b) b and (c) c for two Trombe wall types.
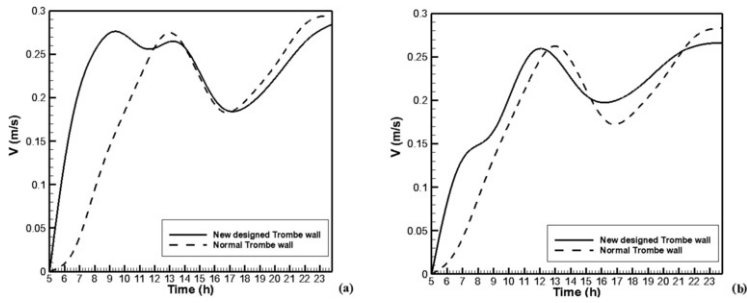
Fig. 15 Average air velocity variation passing through (a) the channel and (b) Trombe wall vent for two Trombe wall types.

Table 5 Average relative humidity in different sections of the test room for two Trombe wall types.

	Type of the Trombe wall	Average relative humidity (%)
Section a	New design	29.5
	Normal	28.3
Section b	New design	30
	Normal	28.8
Section c	New design	29.8
	Normal	28.6

Velocity variation

Similar to temperature and relative humidity analysis, the average velocity variation has been studied in two parts including the Trombe wall vent and the channel. Fig. 15 indicates the velocity variation in these parts. As it is evident from this figure, the velocity variation is directly related to solar intensity. As time goes on, the temperature difference between the channel and the room increases that results in an increase in the natural convection which it in turn leads to an increase in the average air velocity passing through the Trombe wall vent and the channel. In the late hours of the day the solar intensity rate reduces causing the natural convection, consequently, the air velocity to decrease. Due to higher decrease in the room temperature as well as the higher temperature difference between the room and the channel, a dramatic air velocity increase is observed. Performance comparison of two system types revealed that in the morning the new designed Trombe wall results in higher velocity, consequently, higher air ventilation than the normal type in different parts of the system. But, in the normal type there is a delay in establishing the natural air ventilation inside the room (Figs. 12 and 16). With the passage of the time, the normal type indicates higher velocity than the new designed Trombe wall due to the more expansive area of the absorber resulting in higher thermal energy rate transfers to the channel.
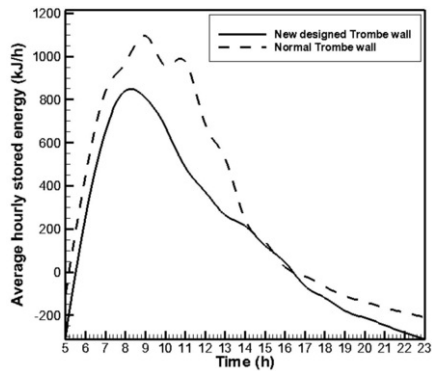
Fig. 16 Stored energy within Trombe wall for two Trombe wall types.

Stored energy analysis

Precise study of Trombe wall performance necessitates stored energy analysis within the Trombe wall. The stored energy is defined as the difference between the energy received by the Trombe wall and the energy transferred from it (Eq. (7)) [27].

$$\dot{E}_{in} - \dot{E}_{out} = \frac{dE}{dt} = stored\ energy \tag{7}$$

Fig. 16 demonstrates the average hourly stored energy amounts. The negative value (happens before sunrise and after sunset) represents the transferred energy from Trombe wall is higher than that received by the Trombe wall. The positive energy value (during the sunshine hours) indicates the reverse condition (Fig. 17).
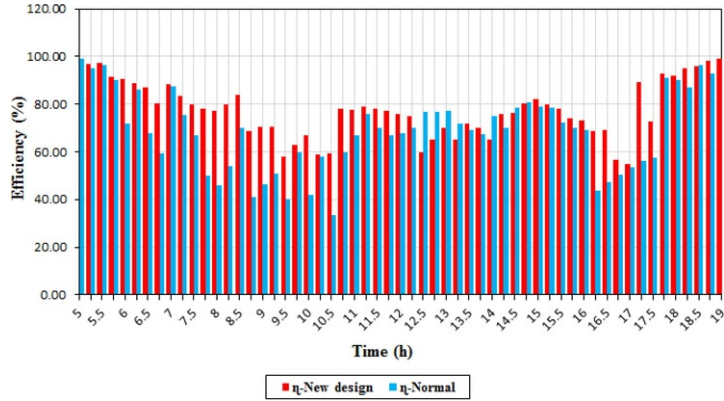

Fig. 17 Average cooling efficiency of two Trombe wall types.

On the basis of obtained results, the average hourly stored energy within the Trombe wall begins to increase when the sun rises and it gradually becomes positive in both Trombe wall types (Fig. 16). Nevertheless the solar intensity is enhanced until 13o'clock, from 10o'clock onwards the stored energy indicates a reduction trend due to increase of temperature difference between the absorber and the channel which it in turn leads to an increase in the difference between the transferred and received energy by the Trombe wall. However, the decreasing trend of stored energy is steeper due to the fact that employing WSS at the incoming fresh air ports decreases the incoming temperature and hereby increases the temperature difference between the absorber and the channel which causes the stored energy to transfer from the Trombe wall to the channel. Consequently, the higher decreasing trend is observed in the presence of water spraying system.

The effect of Trombe wall type on the stored energy analysis indicates that in the morning the energy stored within the new designed Trombe wall is higher than that of normal type, representing the energy received by the new designed Trombe wall is higher than the normal type due to its capability to receive higher solar intensity and to achieve higher absorber temperature. But, from 7o'clock to 17o'clock the energy stored within the normal type transcends because of the more expansive area of its absorber.

Cooling efficiency of the system

Productivity and efficiency play a key role in the analysis of a cooling system performance. The efficiency analysis of Trombe wall cooling performance necessitates the calculation of natural convection heat transfer inside the channel and the solar intensity absorption. The Eq. (8) represents the heat transferred to the air flow through the natural convection in the channel air gap [18]:

$$Q_0 = \dot{m}C_{pf}(T_0 - T_i)$$
$$C_{pf} = [1.007 + 0.00004(T_f - 300)] \times 10^3 \tag{8}$$

The mean air temperature is calculated from [18]:

$$T_f = \gamma T_0 + (1 - \gamma)T_i \tag{9}$$

In these equations, γ is the mean temperature approximation coefficient, taken as 0.74, as suggested by Ong and Chow [32]. In addition, T_i can be taken as equal to the room temperature (T_r). Consequently, the useful heat transferred to the passing air flow can be rewritten in terms of the mean and inlet air temperatures, as given below [18]:

$$Q_0 = \dot{m}C_{pf}(T_f - T_r)/\gamma \tag{10}$$

The thermal efficiency represents the useful energy gained by the air flows through the air channel. Given the temperature rise and the flow rate through the inlet and outlet, the thermal efficiency can be calculated, just as the total heat input can be evaluated as [33]:

$$Q_{tot.} = Q_0 + Q_r \tag{11}$$

The cooling thermal efficiency of the system is given by [33]:

$$\eta = \frac{Q_0}{Q_0 + Q_r} \tag{12}$$

The cooling efficiency of the system has been computed, and according to the results, the cooling efficiency of the new designed type is more than the normal type in 5–8o'clock and 14–16o'clock due to the absorption of solar intensity from side glasses of the channel and, hereby, enhancement of natural convection heat transfer inside the channel. However, the cooling efficiency of the normal type surpasses in midday due to the more expansive area of its absorber and higher stored energy respectively. The daily average cooling efficiency of the new designed Trombe wall is higher than the normal type by around 8.63% (Fig. 17).

Conclusion

A numerical study was carried out to compare the performance of the new designed and normal Trombe walls in terms of temperature, relative humidity and air velocity variation in different parts of the system as well as its cooling efficiency. The obtained results are as follows:

- Based on the ACS evaluation, the thermal comfort conditions for both new designed and normal Trombe walls are properly satisfied. However, the new designed Trombe wall results in approximately lower average temperature inside the room.

- The average room temperature in the new designed Trombe wall is lower than the normal type by around 2 °C.

- Performance comparison of two Trombe wall types discloses that in the morning the new designed Trombe wall results in higher velocity, consequently, higher air ventilation than the normal type in different parts of the system. But, in the normal type there is a delay in establishing the natural air ventilation inside the room. With the passage of the time, the normal type demonstrates higher velocity than the new designed Trombe wall due to the more expansive area of the absorber resulting in higher thermal energy rate transfers to the channel.

- Effect of Trombe wall type on the stored energy analysis indicates that in the morning the energy stored within the new designed Trombe wall is higher than that of normal type, representing the energy received by the new designed Trombe wall is higher than the normal type due to its capability to receive higher solar intensity and to achieve higher absorber temperature. But, from 7o'clock to 17o'clock the energy stored within the normal type transcends because of the more expansive area of its absorber.

- The daily average cooling efficiency of the new designed Trombe wall is higher than the normal type by around 8.63%.

- In overall, the new designed Trombe wall has more desirable performance than the normal type according to the cooling efficiency results and temperature distribution inside the room. The new designed Trombe wall also expands the indoor space and decreases the implementation cost of the Trombe wall.

Acknowledgements

References

[1] W. Liping and L. Angui, A numerical study of trombe Wall for enhancing stack ventilation in building, The 23rd Conference on Passive and Low Energy Architecture, Geneva, Switzerland, 2006.

[2] A. Fernández-González, Analysis of the thermal performance and comfort conditions produced by five different passive solar heating strategies in the United States midwest, *Sol Energy* **81**, 2007, 581–593.

[3] W.I. Okonkwo and C.O. Akubuo, Trombe wall system for poultry brooding, *Int J Poult Sci* **2**, 2007, 125–130.

[4] B. Chen, H.J. Chen, S.R. Meng, X. Chen, P. Sun and Y.H. Ding, The effect of Trombe wall on indoor humid climate in Dalian China, *Renew Energy* **31**, 2006, 333–343.

[5] M. Rabani, V. Kalantar, K.A. Faghih, M. Rabani and R. Rabani, Numerical simulation of a Trombe wall to predict the energy storage rate and time duration of room heating during the non-sunny periods, *Heat Mass Transfer* **49**, 2013, 1395–1404.

[6] A.J.N. Khalifa and E.F. Abbas, A comparative performance study of some thermal storage materials used for solar space heating, *Energy Build* **41**, 2009, 407–415.

[7] J. Khedari, S. Kaewruang, J. Hirunlabh and N. Pratinthong, Natural ventilation of houses by Trombe wall, *Int J Ambient Energy* **20**, 1999, 85–94.

[8] Y. Li, X. Duanmu, Y. Sun, J. Li and H. Jia, Study on the air movement character in solar wall system, 2007, Build. Simul. Beijing; China.

[9] Rabani M. Numerical analysis on performance of a Trombe wall in dry weather (Yazd), Master thesis; 2011.

[10] S. Jaber and S. Ajib, Optimum design of Trombe wall system in mediterranean region, *Sol Energy* **85**, 2011, 1891–1898.

[11] F. Stazi, A. Mastrucci and C. di Perna, The behaviour of solar walls in residential buildings with different insulation levels: an experimental and numerical study, *Energy Build* **47**, 2012, 217-229.

[12] G. Gan, A parametric study of trombe walls for passive cooling of buildings, *Energy Build* **17**, 1998, 37-43.

[13] R. Bassiouny and N.S.A. Koura, An analytical and numerical study of solar chimney use for room natural ventilation, *Energy Build* **40**, 2008, 865-873.

[14] C. Afonso and A. Oliveira, Solar chimneys: simulation and experiment, *Energy Build* **32**, 2000, 71-79.

[15] S.A.M. Burek and A. Habeb, Air flow and thermal efficiency characteristics in solar chimneys and Trombe Walls, *Energy Build* **39**, 2007, 128-135.

[16] H.F. Nouanégué, L.R. Alandji and E. Bilgen, Numerical study of solar-wind tower systems for ventilation of dwellings, *Renew Energy* **33**, 2008, 434-443.

[17] K.E. Amori and S.W. Mohammed, Experimental and numerical studies of solar chimney for natural ventilation in Iraq, *Energy Build* **47**, 2012, 450-457.

[18] N.K. Bansal, J. Mathur, S. Mathur and M. Jain, Modeling of window-sized solar chimneys for ventilation, *Energy Build* **40**, 2005, 1302-1308.

[19] J. Mathur, N.K. Bansal, S. Mathur, M. Jain and Anupma, Experimental investigations on solar chimney for room ventilation, *Sol Energy* **80**, 2006, 927-935.

[20] B. Zamora and A.S. Kaiser, Optimum wall-to-wall spacing in solar chimney shaped channels in natural convection by numerical investigation, *Appl Therm Eng* **29**, 2009, 762-769.

[21] M. Maerefat and A.P. Haghighi, Natural cooling of stand-alone houses using solar chimney and evaporative cooling cavity, *Renew Energy* **35**, 2010, 2040-2052.

[22] J. He, A. Okumura, A. Hoyano and K. Asano, A solar cooling project for hot and humid climates, *Sol Energy* **71**, 2001, 135-145.

[23] S. Chungloo and B. Limmeechokchai, Utilization of cool ceiling with roof solar chimney in Thailand: the experimental and numerical analysis, *Renew Energy* **34**, 2009, 623-633.

[24] R. Rabani, K.A. Faghih, M. Rabani and M. Rabani, Numerical simulation of an innovated building cooling system with combination of solar chimney and water spraying, *Heat Mass Transf* **50**, 2014, 1609-1625.

[25] R. Belarbi, C. Ghiaus and F. Allard, Modeling of water spray evaporation: application to passive cooling of buildings, *Sol Energy* **80**, 2006, 1540-1552.

[26] H. Saffari and S.M. Hosseinnia, Two-phase Euler-Lagrange CFD simulation of evaporative cooling in a Wind Tower, *Energy Build* **41**, 2009, 991-1000.

[27] M. Rabani, V. Kalantar, A.A. Dehghan and K.A. Faghih, Empirical investigation of the cooling performance of a new designed Trombe wall in combination with solar chimney and water spraying system, *Energy Build* **102**, 2015, 45-57.

[28] Z. Yilmaz and Kundakci A. Basak, An approach for energy conscious renovation of residential buildings in Istanbul by Trombe wall system, *Build Environ* **43**, 2008, 508-517.

[29] K. Hami, B. Draoui and O. Hami, The thermal performances of a solar wall, *Energy* **39**, 2012, 11–16.

[30] A. Chel, J.K. Nayak and G. Kaushik, Energy conservation in honey storage building using Trombe wall, *Energy Build* **40**, 2008, 1643–1650.

[31] G. Brager and R. de Dear, A standard for natural ventilation, *ASHRAE J* **42**, 2000, 21–28.

[32] K.S. Ong and C.C. Chow, Performance of solar chimney, *Sol Energy* **74**, 2013, 1–17.

[33] Y. Li and S. Liu, Experimental study on thermal performance of a solar chimney combined with PCM, *Appl Energy* **114**, 2014, 172–178.

Highlights

- A Trombe wall with solar chimney and water spraying system is numerically studied.

- New designed Trombe wall expands room space and decreases its implementation cost.

- The average room temperature in the new designed type is lower than the normal type.

- The cooling efficiency of new designed type is higher than the normal type.